# Extreme Hardening of PDMS Thin Films Due to High Compressive Strain and Confined Thickness

**ARTICLE** *in* LANGMUIR · JUNE 2011

Impact Factor: 4.46 · DOI: 10.1021/la201122e · Source: PubMed



**3 AUTHORS:**

Wenwei Xu
Georgia Institute of Technology
**12** PUBLICATIONS **243** CITATIONS
SEE PROFILE

Nadeen O. Chahine
North Shore-LIJ Health System
**51** PUBLICATIONS **860** CITATIONS
SEE PROFILE

Todd Sulchek
Georgia Institute of Technology
**65** PUBLICATIONS **1,682** CITATIONS
SEE PROFILE

Langmuir

ARTICLE

pubs.acs.org/Langmuir

# Extreme Hardening of PDMS Thin Films Due to High Compressive Strain and Confined Thickness

Wenwei Xu,[†] Nadeen Chahine,[‡] and Todd Sulchek*[,†]

[†]George W. Woodruff School of Mechanical Engineering, Georgia Institute of Technology, Atlanta, Georgia 30332, United States

[‡]Feinstein Institute for Medical Research, 350 Community Drive, Manhasset, New York 11030, United States

**ABSTRACT:** Polymers confined to small dimensions and that undergo high strains can show remarkable nonlinear mechanics, which must be understood to accurately predict the functioning of nanoscale polymer devices. In this paper we describe the determination of the mechanical properties of ultrathin polydimethylsiloxane (PDMS) films undergoing large strains, using atomic force microscope (AFM) indentation with a spherical tip. The PDMS was molded into extremely thin films of variable thickness and adhered to a hard substrate. We found that for films below 1 $\mu$m in thickness the Young's modulus increased with decreasing sample thickness with a power law exponent of 1.35. Furthermore, as the soft PDMS film was indented, significant strain hardening was observed as the indentation depth approached 45% of the sample thickness. To properly quantify the nonlinear mechanical measurements, we utilized a pointwise Hertzian model which assumes only piecewise linearity on the part of the probed material. This analysis revealed three regions within the material. A linear region with a constant Young's modulus was seen for compression up to 45% strain. At strains higher than 45%, a marked increase in Young's modulus was measured. The onset of strain induced stiffening is well modeled by finite element modeling and occurs as stress contours expanding from the probe and the substrate overlap. A third region of mechanical variation occurred at small indentations of less than 10 nm. The pointwise Young's modulus at small indentations was several orders of magnitude higher than that in the linear elasticity region; we studied and ruled out causes responsible for this phenomenon. In total, these effects can cause thin elastomer films to become extremely stiff such that the measured Young's modulus is over a 100-fold higher than the bulk PDMS. Therefore, the mechanics of a polymer can be changed by adjusting the geometry of a material, in addition to changing the material itself. In addition to understanding the mechanics of thin polymer films, this work provides an excellent test of experimental techniques to measure the mechanics of other nonlinear and heterogeneous materials such as biological cells.

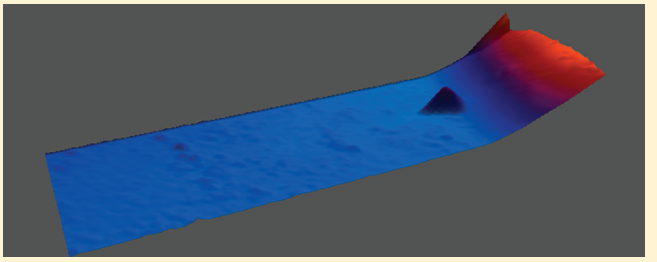

## INTRODUCTION

PDMS (polydimethylsiloxane) and other soft elastomeric polymers are frequently constructed with micrometer dimensions for use in many science and engineering applications.[1−4] As small deformations of PDMS within microdevices can impact their function,[5,6] understanding how strain and geometry affect the mechanical properties of PDMS is of considerable relevance.[7,8] However, few studies have investigated PDMS mechanics at the micro/nanoscale, where small displacements can lead to significant deformations comparable to the size of the sample, leading to significant modulations of the mechanics of the polymer.

Indentation of thin films and biomaterials with the atomic force microscope (AFM) is a widely used method to characterize mechanical properties.[9−12] To properly quantify the mechanical properties from the force−indentation curves, researchers apply various models, which include the Hertz model, JKR model, and DMT model, to obtain a Young's modulus.[13−15] However, indentation of materials defined by nanoscale dimensions differs from traditional indentation in that small deformations of geometrically confined materials can lead to deviations from the properties of bulk materials.[16−20]

The objective of this research is to probe ultrathin PDMS films upon hard substrates to determine the effect of the geometry (thickness of the film), the applied strain, and the interfacial surface phenomena on the measured mechanical properties. In previous studies of thin PDMS films, the polymer films used were at least 10 $\mu$m in thickness,[19,20] which prohibited exploration of very high strains (>45%) in which strongly nonlinear behavior is significant. In this study, we probe PDMS films which have thicknesses ranging from 43 nm to 1 $\mu$m. These ultrathin elastomer films allow us to generate significant strains of over 50%. The large compressive strains reveal highly nonlinear mechanical behavior. Consequently, we have employed a pointwise model, developed first by Costa,[10] to analyze the indentation-dependent stiffness of ultrathin PDMS without any assumptions of linearity of the polymer and therefore can be used to quantitatively describe the strain-dependent stiffness. The experimentally determined indentation dependent Young's modulus plots obtained agreed

**Received:** March 25, 2011
**Revised:** May 16, 2011
**Published:** June 02, 2011

with the finite element modeling (FEM) simulations of PDMS thin films upon an underlying glass substrate.

We explore the response of ultrathin PDMS films in three regions: contact, small deformation, and large deformation ranges. We find that at small deformations (strain <45%) the modulus increased to the 1.35 power as the sample thickness decreased. The modulus value gradually approached the value for the bulk sample for film thickness greater than 900 nm. In the large deformation range, the Young's modulus abruptly increases with indentation, indicating significant strain hardening. In addition to the stiffening due to geometry and strain, previous studies have shown that the point of contact results in extremely high values of Young's modulus.[21−23] This phenomenon of contact stiffening occurs over very small indentations of a few nanometers. On the basis of our pointwise analysis of thin polymer films, we show that the contact stiffening phenomenon is not due to probe−sample adhesion.

## EXPERIMENT PROCEDURES

**Sample Preparation.** The thin PDMS film used in this research was fabricated using Sylgard 184 Silicone Elastomer Kit from Dow Corning. The mixture of two components was placed in a vacuum chamber to remove the gas in the mixture and then poured between two angled glass slides to form a PDMS film of decreasing thickness at the end. The curing process took place in an oven at 60 °C for 30 min. The top slide was carefully separated to reveal a thin PDMS film with slightly varying thickness bonded to a glass substrate, as shown in Figure 1a. The thickness of the film at the locations of the indentation was determined by AFM topography measurement. The thickness for the experiment was measured to be 43−90 nm and shown schematically as locations A−D in Figure 1a. In addition, thicker PDMS samples were investigated (1000 nm and greater), though the thickness was measured with optical microscopy. The nanoindentation experiment conducted on samples of different thicknesses investigated the dependence of the force response on sample thickness.

**Atomic Force Microscope Imaging and Stiffness Measurements.** The AFM (Asylum MFP-3D) was used for both imaging of the polymer films and for polymer mechanics measurements. Cantilevers from Olympus (Model #:AC160TS) were used as indenters. To simplify the contact geometry between the indenter and the PDMS sample, the cantilever was modified by attaching a silica microsphere on the tip, as shown in Figure 1b. The nominal value of the microsphere diameter is 4.74 $\mu$m. The modified cantilever indenter was calibrated on the glass substrate and the spring constant was determined as 61.0 N/m using the thermal vibration method,[24] in which a Lorentzian function was used to fit the thermal noise spectrum. In all experiments, the deflection of the cantilever did not exceed the linearity of the photosensitive detector, even for forces up to 16 $\mu$N. AFM was combined with an inverted optical bright field microscope (Nikon Ti-U) to align the cantilever to the PDMS sample. Samples of different thicknesses used in this study include 43, 52, 70, 90, and 1000 nm. Bulk PDMS samples (thickness values much greater than a micrometer) were also studied for comparison.

**Modified Hertz Model and JKR Model.** The Hertz model is widely used in contact mechanics research.[15,25] Hertz derived this model to describe the normal contact between two deformable spheres, and the model has been adapted for other contact geometries as well.[25,26] The mathematical expressions of the Hertz model for two deformable spheres are of the form described in eqs 1 and 2.

$$a^3 = \frac{3PR}{4E^*} \tag{1}$$

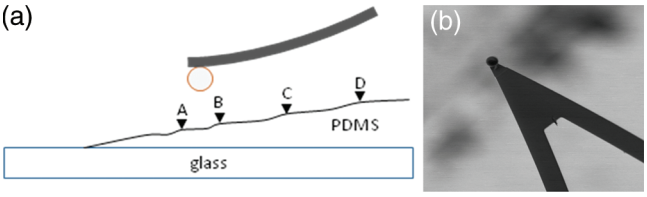


**Figure 1.** (a) Experimental configuration of the mechanical measurement. (b) A beaded cantilever tip that is similar to that used in this study.

$$\delta = \left(\frac{9P^2}{16RE^{*2}}\right)^{1/2} \tag{2}$$

where $a$ is the radius of the contact region between the indenter and the sample, $\delta$ is the indentation into the material, $P$ is the loading force, and $R$ is the effective radius of curvature defined as $1/R = 1/R_1 + 1/R_2$, $E^*$ is the apparent Young's modulus defined as $1/E^* = (1 - \nu_1^2)/E_1 + (1 - \nu_2^2)/E_2$, where $\nu_1$ and $\nu_2$ are the Poisson's ratio for the material and the subscripts denote the two contacting bodies. The radius of curvature of the PDMS surface at the indentation locations was obtained by AFM imaging. By analyzing the specific cross sectional profile of the topography, we determined the radius of curvature. The smallest radius of curvature of the PDMS surface at the indentation locations is 24 $\mu$m, which is 10 times larger than the radius of the indenter; thus, we simplify $R$ to $R_1$, which is the radius of the microsphere used in this study.

The Hertz model assumes linear elasticity, which is typically valid when the indentation is small compared to the sample thickness (small strain). However, PDMS is a hyperelastic material and can elastically undergo large nonlinear deformations. In this case, the assumption is not valid and the Hertz model will not accurately predict the mechanical response of the material. To obtain the pointwise Young's modulus, we follow the methodology developed by Costa et al.[13] Briefly, each data point ($\delta_i$, $P_i$) in the indentation−force curve obtained from experiments was substituted into eq 2 to calculate the corresponding $E_i^*$. The pointwise Young's modulus $E^*$ versus indentation $\delta$ can then be plotted.

In order to examine the contact response of ultrathin PDMS, we employed the JKR (Johnson−Kendall−Roberts) model to determine the effect of adhesion force on contact conformations. The mathematical expressions for the JKR model are shown in eqs 3 and 4, where $\sigma$ is the surface energy between indenter and sample and the other parameters are the same as described previously.

$$a^3 = R/E^*(P + 3\sigma\pi R + \sqrt{(6\sigma\pi RP + [(3\sigma\pi R)]^2)}) \tag{3}$$

$$E^* = \frac{\left(\frac{2}{3}P\right)^{3/2}}{\delta^{3/2}R^{1/2}[P + 3\sigma\pi R + \sqrt{6\sigma\pi RP + (3\sigma\pi R)^2}]^{1/2}} \tag{4}$$

When the indentation is small, the adhesion force plays an important role in deforming the contact conformation[15] and hampering interpretation of the data. However, as the indentation increases, the significance of the adhesion force decreases and the JKR model will typically approach the Hertz model in describing contact behavior between the indenter and sample.

**Finite Element Simulation.** We also used the finite element analysis (FEA) simulation software Abaqus from SIMULIA to simulate PDMS contact mechanics for comparison with the experimental measurements. We follow the work of previous researchers.[10] The PDMS film was modeled as a planar, axisymmetric mesh. The silica bead was


dx.doi.org/10.1021/la201122e |Langmuir 2011, 27, 8470–8477

modeled as a rigid body, with a diameter of 4.74 $\mu$m, which contacts the PDMS mesh during the course of simulation. The bottom of the PDMS mesh was fixed in position to simulate adherence to the substrate. To capture the hyperelasticity of PDMS during the large deformation of our experiments, we used the Mooney–Rivlin model[27] which is appropriate for rubber-like materials undergoing large deformations.[18] For incompressible hyperelastic materials, the model derives the stress–strain relationship from the expression $W = C_1(I_1 - 3) + C_2(I_2 - 3)$, where $W$ is the strain energy function, $I_1$ = trace($\mathbf{G}$), and $I_2$ = (trace($\mathbf{G}$) − trace($\mathbf{G}^2$))/2, where $\mathbf{G}$ is the right Cauchy–Green deformation tensor defined as $\mathbf{G} = \mathbf{F}\mathbf{F}^T$, with $\mathbf{F}$ as the deformation gradient tensor. $C_1$ and $C_2$ are material constants, which were obtained by fitting the experimental force versus indentation curve of the 90 nm thick film and then input into Abaqus to model the other thicknesses. The indentation depths used in the simulation were identical to the experimental values.

## RESULTS AND DISCUSSION

The results for nanoindentation of ultrathin PDMS films are shown and compared in Figure 2. Individual force versus indentation curves for 43, 52, 70, and 90 nm thick PDMS samples are plotted on the same scale. From these data, it is clear that the slope at a given indentation increases with decreasing film thickness.

Figure 3 compares the experimental data to both a Hertzian contact model of force indentation by an indenter as well as a FEA simulation of a thin elastomer in compression. The experimental force curves and the FEA simulations closely match over the whole indentation range for all polymer thicknesses. The FEA results do show slight deviations in regions, which may be due to other factors not taken into account in the model, such as friction between the sample and the indenter due to probe adhesion.[28] Also from Figure 3, we see that the Hertz model does not accurately describe the relationship between force and indentation for PDMS compression over large strain values. It is apparent that the Hertz model is initially relatively accurate but deviates from the experimental data at indentation greater than 45% of the film thickness. This result is not surprising in light of the fact that even small indentations of thin polymer films on a hard substrate will cause large strains and an apparent hardening and has been described in several previous articles.[16,17,29]

**Pointwise Young's Modulus versus Thickness.** The stiffness of nonlinear materials can be empirically determined by fitting the Hertz model to sections of the force versus indentation curve to calculate a pointwise Young's modulus.[10] The pointwise Young's modulus plotted as a function of indentation (Figure 4) determines the amount of deformation at which point nonlinearity in the stiffness emerges. We highlight three regions of interest in the modulus–indentation relationship of PDMS samples with different thicknesses, identified by three partitions separated by indentation values $\delta_1$ and $\delta_2$. Region 1 is characterized by a constant Young's modulus independent of indentation; in region 2, the Young's modulus increases with indentation, indicating an increasing stiffness; and in region 3 (i.e., immediately post contact), the Young's modulus initially shows a very high value upon contact and then drops drastically to a constant level. For an indentation depth within region 1, the pointwise elastic modulus was found to be nearly constant with indentation for each sample; therefore, the mechanical behavior is linear, and the Hertz model is applicable to this indentation range. As the indentation increases to region 2, the effect of underlying hard substrate becomes appreciable and gradually dominates the measured mechanical stiffness. This fact is consistent with the results shown in Figure 3.

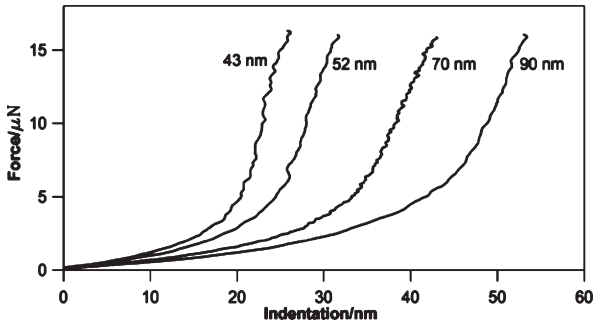


**Figure 2.** Force versus indentation curves for 45, 52, 70, and 90 nm thick PDMS samples.

We define $\delta_2$ as a transition point from linearity to nonlinearity based upon a change of slope of the modulus–indentation plot. We find the value of $\delta_2$ to be dependent on sample thickness. As shown in Figure 5, the transition points are plotted versus thicknesses. The slope of the line obtained from linear regression fitting is 0.4533 ($R^2$ value is 0.9999), meaning that the linear elasticity region occurs until the indentation approaches 45% of the thickness.

To explain the onset of an increased modulus in region 2 at a consistent strain, we carefully scrutinize the stress evolution in the FEA simulation. Figure 6 shows the stress evolution for the 90 nm PDMS thin film. As the indenter compresses the PDMS film, increased stress contours develop at both the indenter–sample interface and also at the PDMS–substrate interface. For moderate indentations ($\delta < \delta_2$), these two zones of increased stress were not in physical contact, leading to a constant pointwise Young's modulus as the region of low stress remained. However, as the indentation increased to 33% of film thickness, these two zones of increased stress gradually converge. As the indentation reaches 45% of the film thickness, high stress values fully develop throughout the region between the indenter and substrate, coinciding with an increase in the pointwise modulus. We carried out FEM simulations for other sample thicknesses and observed a similar evolution of stress contours with increasing indentation, culminating in a uniform high stress at 45% indentation for all sample thicknesses, consistent with the experimental results.

As we show in Figure 4, the compressive elastic modulus in region 1 increases with decreasing PDMS thickness. To quantify the dependence of the elastic modulus to sample thickness, we implemented the same nanoindentation experiment on a 1 $\mu$m thick sample and a bulk PDMS sample. The pointwise Young's modulus versus indentation plots for these two thicknesses are shown in Figure 7. The elastic modulus of the 1 $\mu$m thick PDMS sample in the linear elasticity region 1 is identical to that of the bulk sample. We also note that the 1 $\mu$m thick PDMS layer also shows a significant increase in the pointwise elastic modulus at 45% strain, consistent with what we have observed from the ultrathin PDMS samples. Comparing the moduli in region 1, denoted by $E_1$, for the range of sample thicknesses, we see a quantitative dependence of elastic modulus in region 1 on sample thickness. To investigate the dependence of $E_1$ on sample thickness, we plot $E_1$ versus sample thickness. As shown in Figure 8, $E_1$ is found to be inversely proportional to $(\text{thickness})^{-1.35}$ ($R^2$ value is 0.9852), with the elastic modulus converging to that of bulk at a PDMS thicknesses greater than 900 nm.

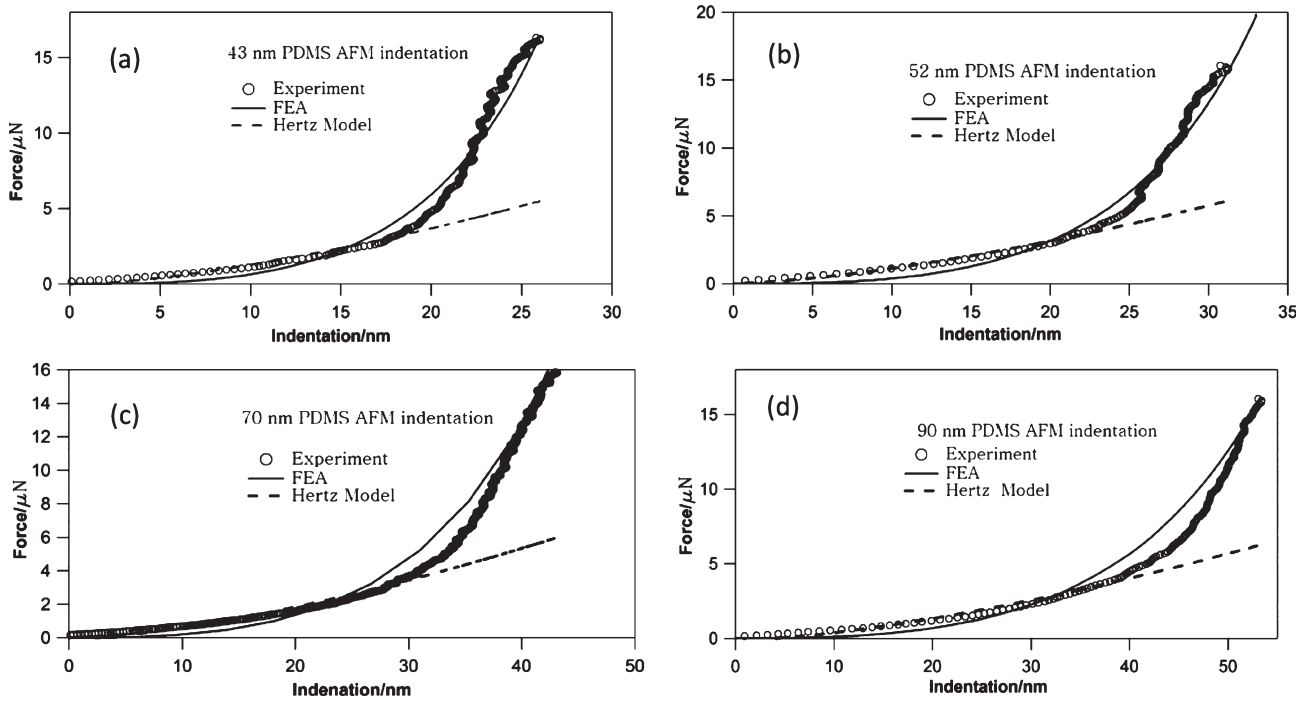


**Figure 3.** Experimental force curves and FEA simulation results for PDMS films for (a) 43, (b) 52, (c) 70, and (d) 90 nm samples.

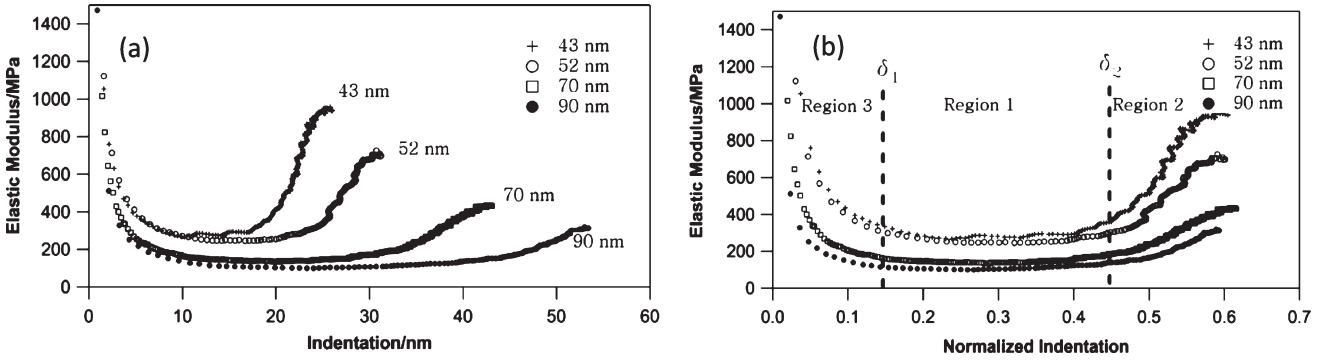


**Figure 4.** Pointwise Young's modulus versus (a) indentation and (b) normalized indentation for 45, 52, 70, and 90 nm thick PDMS samples.

The dependence of stiffness on size has also been reported for tensile electrospun nanofibers,[30] in which the elastic modulus increases abruptly when the diameter of the nanofiber decreases to a certain threshold.[30] Previous literature[31,32] also reported the power relationship between the Young's modulus and thickness for polymeric films, although these studies studied films several orders of magnitude higher in thickness and found a dependence on $(\text{thickness})^{-0.5}$. O'Connell and Mckenna found a dramatic stiffening of poly(vinyl acetate) film in rubbery region, and the stiffness scales with approximately $(\text{thickness})^{-2}$;[33] Xu and Mckenna also showed that the Young's modulus of ultrathin poly(butyl methacrylate) films scales with $(\text{thickness})^{-1}$;[34] Rowland and co-workers also found the stiffening of layers compared to bulk polystyrene.[35] Although we did not investigate this discrepancy in the index, we do expect that surface tension, also known as residual stress, will play a significant role in the mechanics as the ratio of surface area to volume becomes large and may be a factor contributing to the increasing of Young's modulus with decreasing thickness.[36,37] If this interpretation is correct, our data suggest negligible contribution from surface tension to occur at 900 nm, and thus the Young's modulus of the thin film approaches the value for bulk material.

**Pointwise Young's Modulus in Small Indentation Region (Region 3).** A remarkable observation seen in the pointwise Young's modulus plots is the extremely high values for elastic modulus for initial indentation, denoted as region 3. This observation has been reported in previous studies,[21−23] and the result is puzzling as the elastic modulus is calculated to be orders of magnitude higher than the value for the elastic modulus in region 1. We have investigated this phenomenon by adjusting several experimental parameters and excluded these factors as an entire explanation. Even by accounting for probe adhesion and misidentification of the contact point, we continue to measure a contact-dependent change in modulus.

Probe−sample adhesion can lead to significant deviation of the expected contact area determined from the Hertz model,


dx.doi.org/10.1021/la201122e |*Langmuir* 2011, 27, 8470–8477

resulting in an artificially high pointwise Young's modulus. As surface energy plays an important role in nanoscale contact mechanics,[15] it can conceivably lead to extremely high measured modulus in the small indentation region. We developed a pointwise JKR (Johnson, Kendall, Roberts) model[15] to account for the effect of probe−sample surface energy on the pointwise Young's modulus. The probe−sample surface energy was determined from a subsequent adhesion measurement to the compressive modulus measurement.[38] As expected, the measured modulus is drastically reduced at small indentations, but significant contact stiffening remains (Figure 9). To confirm that probe adhesion is not leading to an artificially high modulus, we repeated the experiment in deionized water to eliminate capillary forces, which can apply several nanonewtons of adhesive force leading to significant deviation from Hertzian assumptions.

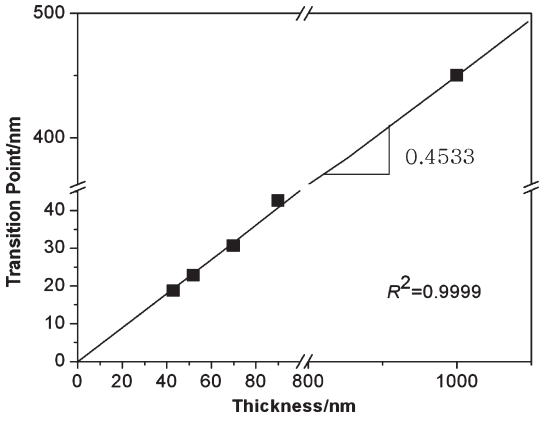


**Figure 5.** Plot showing the indentation of transition from region 1 to region 2 ($\delta_2$) versus PDMS thickness.

Using the pointwise JKR model and a liquid measurement environment, the measured pointwise elastic modulus in region 3 still exceeds the elastic modulus in region 1 by several orders of magnitude. Accounting for and reducing the adhesive forces between the sample and indenter cannot explain the extremely high modulus in region 3.

To rule out viscoelastic effects that may account for the contact stiffening, we also varied the loading speed of the indentation process, which had no effect on the modulus. The indenting loading speed was tested at 12.8, 9.4, 4.6, 1.7, and 0.87 $\mu$m/s, and the results show no effect of loading speed on the elastic modulus as indicated in the inset of Figure 9. The measurements were performed at the same location on the bulk PDMS, and the pointwise JKR model was used to eliminate the influence of surface energy on the result. Surface viscoelasticity has been investigated for other materials, and the results show a close agreement with the published data for bulk materials.[39] Because

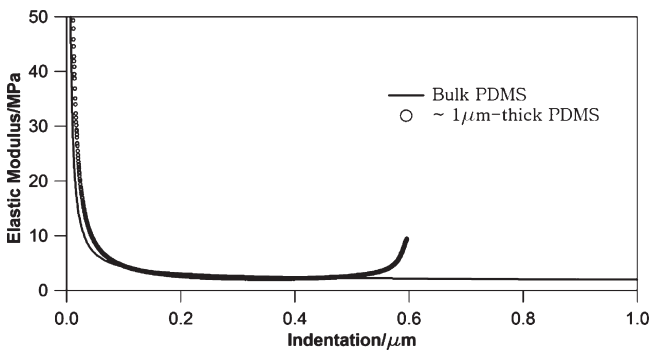


**Figure 7.** Plot showing pointwise Young's modulus versus indentation for 1 $\mu$m thick and bulk PDMS.

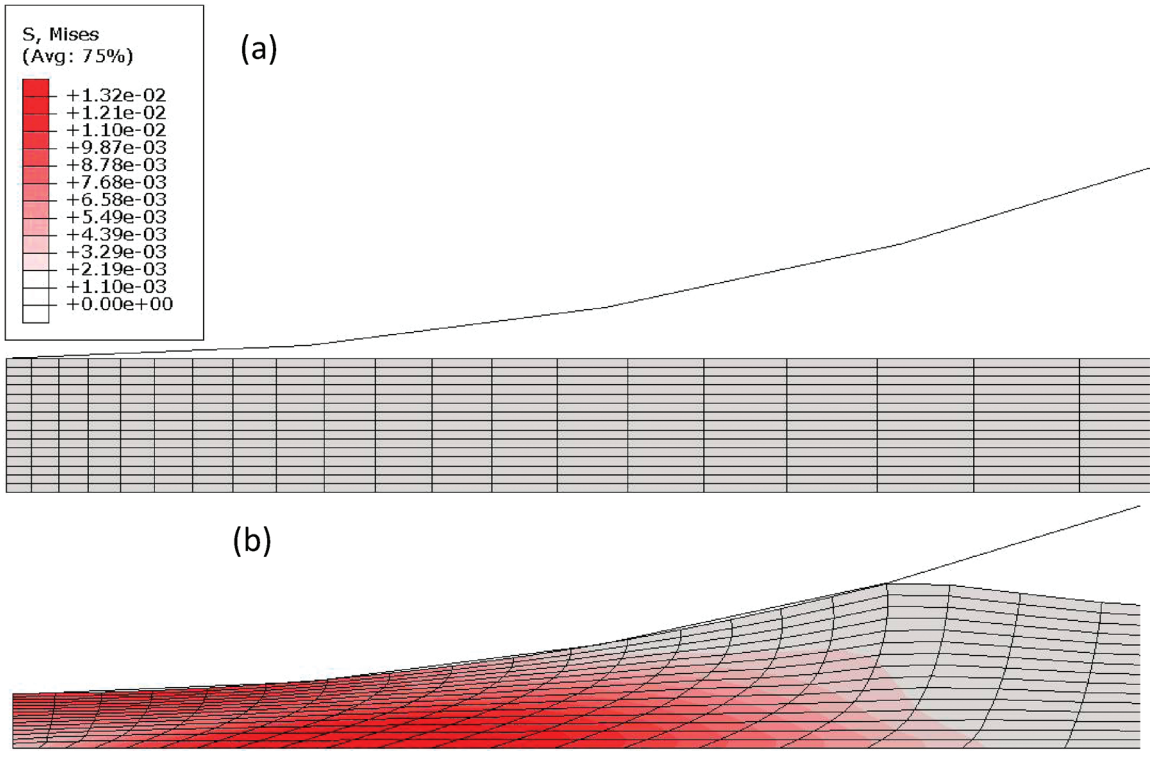


**Figure 6.** Evolution of stress (in GPa) in the 90 nm thick PDMS sample in the FEA simulation (a) before and (b) after deformation.


dx.doi.org/10.1021/la201122e |*Langmuir* 2011, 27, 8470–8477

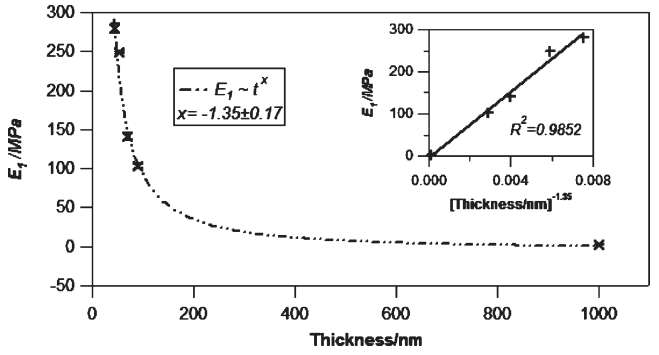


**Figure 8.** Average Young's modulus in region 1 ($E_1$) for different sample thicknesses. The standard deviation for the data is below the size of the markers in this figure. The inset plots $E_1$ as a function of $(\text{thickness})^{-1.35}$.

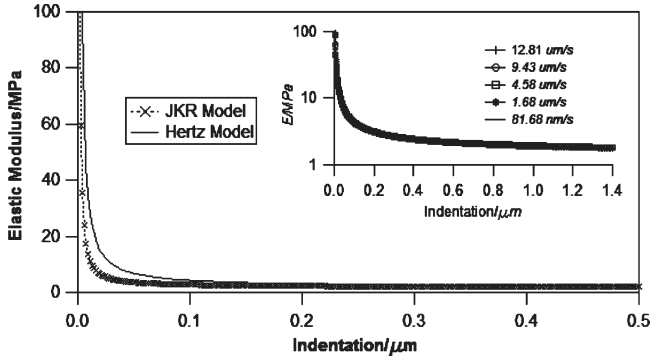


**Figure 9.** Pointwise Young's modulus plots determined using the Hertz and JKR model. The inset shows the effect of loading speed.

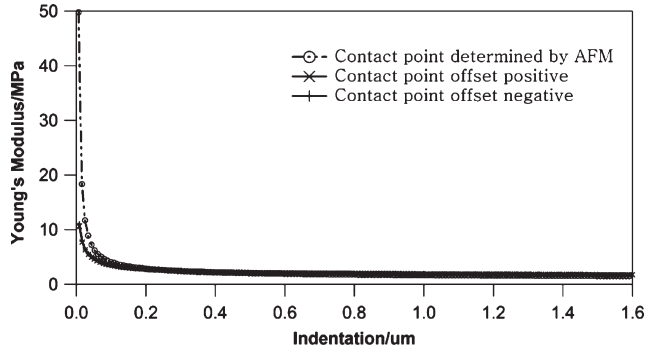


**Figure 10.** Pointwise Young's modulus determined after shifting the contact point to higher and lower values.

of the lack of dependence of modulus on loading rate, we reason that viscoelasticity is not a significant factor causing the high modulus at small indentations.

There is some debate concerning the physical properties of the interfacial region near surface of ultrathin polymer films. Some researchers have suggested the existence of a liquidlike region near the surface of polystyrene films,[40,41] resulting from a lower glass transition temperature than the bulk material, whereas others have shown there to be little or no change in glass transition temperature or existence of the liquid layer.[42] Also, buckling-based methods can be used to determine the elastic moduli of ultrathin polymer films.[43−47] Stafford and co-workers[48] measured the elastic moduli for a series of ultrathin polymer films deposited on thick PDMS substrates. By examining the wrinkling instability of these films and fitting the data with a bilayer model, they found that as the thicknesses of these thin films became smaller, the surface regions of the thin films became softer. In our study, we do not find evidence of the presence of a softer liquid layer in PDMS.

Previous explanations of contact stiffening include the misidentifying of the contact point while determining the pointwise Young's modulus.[12] To investigate the effect of misidentifying the contact point, we purposely shifted the contact point to greater and lesser values while repeated the fitting procedure. As seen in Figure 10, offsetting the contact point both to higher and lower values decreases the Young's modulus in the small indentation region 3 but does not completely eliminate the effect in our measurements. In addition, the offset produces a slightly worse fit of the data for the remaining portion of the force curve. While we have not ruled out the role of accurate identification of the contact point, one alternative explanation of high stiffness includes the role of a unique interfacial region between the indenter and the polymer upon contact and the elevated glass transition temperature $T_g$ with respect to the uncontacted surface.[21] An elevated $T_g$ would shift the interfacial region to a glassy regime, leading to significant stiffening in comparison to rubbery regime. In addition, the reduction of molecular mobility at the interface, which is induced by the attraction between the indenter and surface, could also contribute to the stiffening of the surface.[21] Hydrostatic pressure at the contact interface leading to an elevation of $T_g$ in several other polymers, including polystyrene, poly(methyl methacrylate),[49,50] and polycarbonate,[51] have been reported. For small indentations, the interfacial region dictates the mechanical behavior of the nanoindentation−force response; however, as the indentation increases, the volumetric proportion of the interfacial region decreases as the total volume of strained polymer increases, and thus the contribution of the interfacial region to the overall mechanical response becomes negligible for sufficient indentation.

## CONCLUSION

The mechanical properties of ultrathin PDMS films bonded to a hard glass substrate were studied using AFM. A pointwise Hertz model and JKR model were used to determine the indentation-dependent Young's modulus. The mechanical properties of PDMS thin films were strongly influenced by high strain from compression between the indenter and the underlying substrate and showed an increase in the indentation-dependent Young's modulus at consistent strain values of 45% for all samples studied. In addition, the mechanical properties of PDMS thin films were strongly affected by the thickness of the polymer at all strains. The average Young's modulus in region 1 ($E_1$) increased as the sample thickness decreased and gradually approached the modulus value for bulk sample for a thickness value greater than 900 nm. The experimental mechanical profile was accurately described by FEA simulation over the entire indentation range. The high elastic modulus in region 3 at the indenter−sample interface plays a dominant role in the contact mechanics and quickly becomes negligible as the indentation advances. Contact-dependent stiffness does not seem to be exclusively caused by measurement artifacts, analysis methods, or interfacial adhesion.

The results described here will enable predictive understanding of the mechanical properties of elastomeric materials under large deformations as can occur within microdevices.[52−54] These important properties of PDMS should be considered in device design where nanoscale elastomers undergo large deformations. In addition, the methods described here to reliably characterize nonlinear mechanical materials may also impact the study of other nonlinear materials such as cells. PDMS has some similar mechanical characteristics to single cells, including hyperelasticity and nonlinear elasticity.[55] Cell mechanics studies with AFM of adherent cells often report a stiffening due to the underlying substrate. In these experiments, adherent cells are typically immobilized onto a hard substrate and probed under large strain.[56,57] It is often assumed that the underlying substrate strongly affects the measured mechanical properties, but the effect of material thickness has not been determined quantitatively. The methods described here can likewise be applied to understand heterogeneous and nonlinear materials such as cells, as long as an accurate measurement of cell thickness can be obtained. This research contributes a new perspective on quantifying and interpreting mechanical properties of cells and other nonlinear and thin materials.

## AUTHOR INFORMATION

### Corresponding Author

*E-mail: todd.sulchek@me.gatech.edu. Phone: (404) 385-1887.

## ACKNOWLEDGMENT

This work is funded in part by the National Science Foundation (NSF) (Grant CBET-1027630). The authors sincerely thank Craig Blanchette, Gabriella Loots, Karl Jacob, Ting Zhu, John Lyons, and the anonymous reviewers for useful discussions and suggestions.

## REFERENCES

(1) Shih, T. K.; Chen, C. F.; Ho, J. R.; Chuang, F. T. *Microelectron. Eng.* **2006**, *83*, 2499–2503.
(2) Nam, Y.; Musick, K.; Wheeler, B. C. *Biomed. Microdevices* **2006**, *8*, 375–381.
(3) Nam, Y.; Chang, J. C.; Wheeler, B. C.; Brewer, G. J. *IEEE Trans. Biomed. Eng.* **2004**, *51*, 158–165.
(4) Jo, B. H.; Van Lerberghe, L. M.; Motsegood, K. M.; Beebe, D. J. *J. Microelectromech. Syst.* **2000**, *9*, 76–81.
(5) Zhang, W. *Lab Chip* **2009**, *9*, 3088–3094.
(6) Jeong, O. C.; Konishi, S. *Sens. Actuators, A* **2007**, *135*, 849.
(7) Mata, A.; Fleischman, A. J.; Roy, S. *Biomed. Microdevices* **2005**, *7*, 281–293.
(8) Tambe, N. S.; Bhushan, B. *Ultramicroscopy* **2005**, *105*, 238–247.
(9) Oliver, W. C.; Pharr, G. M. *J. Mater. Res.* **1992**, *7*, 1564–1583.
(10) Costa, K. D.; Yin, F. C. P. *ASME J. Biomech. Eng.* **1999**, *121*, 462–471.
(11) Karduna, A. R.; Halperin, H. R.; Yin, F. C. P. *Ann. Biomed. Eng.* **1997**, *25*, 1009–1016.
(12) S. L. Crick, S. L.; Yin, F. C. P. *Biomech. Model. Mechanobiol.* **2007**, *6*, 199–210.
(13) Costa, K. D.; Sim, A. J.; Yin, F. C. P. *ASME J. Biomech. Eng.* **2006**, *128*, 176–184.
(14) Grierson, D. S.; Flater, E. E.; Carpick, R. W. *J. Adhes. Sci. Technol.* **2005**, *19*, 291–311.
(15) Johnson, K. L.; Kendall, K.; Roberts, A. D. *Proc. R. Soc. London, A* **1971**, *324*, 301–313.
(16) Dimitriadis, E. K.; Horkay, F.; Maresca, J.; Kachar, B.; Chadwick, R. S. *Biophys. J.* **2002**, *82*, 2798–2810.
(17) Domke, J.; Radmacher, M. *Langmuir* **1998**, *14*, 3320–3325.
(18) Lin, D. C.; Dimitriadi, E. K.; Horkay, F. *eXPRESS Polym. Lett.* **2007**, *1*, 576–584.
(19) Jee, A. Y.; Lee, M. *Polym. Test.* **2010**, *29*, 95–99.
(20) Tranchida, D.; Piccarolo, S.; Soliman, M. *Macromolecules* **2006**, *39*, 4547–4556.
(21) Tweedie, C. A.; Constantinides, G.; Lehman, K. E.; Brill, D. J.; Blackman, G. S.; Van Vliet, K. J. *Adv. Mater.* **2007**, *19*, 2540–2546.
(22) Mahaffy, R. E.; Park, S.; Gerde, E.; Käs, J.; Shih, C. K. *Biophys. J.* **2004**, *86*, 1777–1793.
(23) Rico, F.; Roca-Cusachs, P.; Gavara, N.; Farré, R.; Rotger, M.; Navajas, D. *Phys. Rev. E* **2005**, *72*, 021914.
(24) Hutter, J. L.; Bechhoefer, J. *Rev. Sci. Instrum.* **1993**, *64*, 1868–1873.
(25) Johnson, K. L. *Contact Mechanics*; Cambridge University Press: New York, 1985; Chapter 4.
(26) Dintwa, E.; Tijskens, E.; Ramon, H. *Granular Matter* **2008**, *10*, 209–221.
(27) Treloar, L. R. G. *The Physics of Rubber Elasticity*, 2nd ed.; Clarendon Press: Oxford, 1958; Chapter 8.
(28) Zhang, M.; Zheng, Y. P.; Mak, A. F. T. *Med. Eng. Phys.* **1997**, *19*, 512–517.
(29) Saha, R.; Nix, W. D. *Acta Mater.* **2002**, *50*, 23–38.
(30) Arinstein, A.; Zussman, E. *J. Polym. Sci., Part B: Polym. Phys.* **2011**, *49*, 691–707.
(31) Liu, M.; Sun, J.; Sun, Y.; Bock, C.; Chen, Q. *J. Micromech. Microeng.* **2009**, *19*, 035028.
(32) Oommen, B.; Van Vliet, K. J. *Thin Solid Films* **2006**, *513*, 235–242.
(33) O'Connell, P. A.; McKenna, G. B. *Eur. Phys. J. E* **2006**, *20*, 143–150.
(34) Xu, S.; O'Connell, P. A.; McKenna, G. B. *J. Chem. Phys.* **2010**, *132*, 184902.
(35) Rowland, H. D.; King, W. P.; Pethica, J. B.; Cross, G. L. W. *Science* **2008**, *322*, 720–724.
(36) Dingreville, R.; Qu, J.; Cherkaoui, M. *J. Mech. Phys. Solids* **2005**, *53*, 1827–1854.
(37) Cuenot, S.; Frétigny, C.; Demoustier-Champagne, S.; Nysten, B. *Phys. Rev. B* **2004**, *69*, 165410.
(38) Greenwood, J. A.; Johnson, K. L. *J. Phys. D: Appl. Phys.* **1998**, *31*, 3279–3290.
(39) Houston, J. E. *J. Polym. Sci., Part B: Polym. Phys.* **2005**, *43*, 2993–2999.
(40) Teichroeb, J. H.; Forrest, J. A. *Phys. Rev. Lett.* **2003**, *91*, 016104.
(41) Fakhraai, Z.; Forrest, J. A. *Science* **2008**, *319*, 600–604.
(42) Hutcheson, S. A.; McKenna, G. B. *Phys. Rev. Lett.* **2005**, *94*, 076103.
(43) Stafford, C. M.; Harrison, C.; Beers, K. L.; Karim, A.; Amis, E. J.; Vanlandingham, M. R.; Kim, H. C.; Volksen, W.; Miller, R. D. *Nature Mater.* **2004**, *3*, 545–550.
(44) Nolte, A. J.; Rubner, M. F.; Cohen, R. E. *Macromolecules* **2005**, *38*, 5367–5370.
(45) Stafford, C. M.; Guo, S.; Harrison, C.; Chiang, Y. M. *Rev. Sci. Instrum.* **2005**, *76*, 062207.
(46) Nolte, A. J.; Cohen, R. E.; Rubner, M. F. *Macromolecules* **2006**, *39*, 4841–4847.
(47) Wilder, E. A.; Guo, S. L.; Gibson, M. J.; Fasolka, M. J.; Stafford, C. M. *Macromolecules* **2006**, *39*, 4138–4143.
(48) Torres, J. M.; Stafford, C. M.; Vogt, B. D. *ACS Nano* **2009**, *3*, 2677–2685.
(49) Alcoutlabi, M.; McKenna, G. B. *J. Phys.: Condens. Matter* **2005**, *17*, R461–R524.
(50) Gacoin, E.; Fretigny, C.; Chateauminois, A.; Perriot, A.; Barthel, E. *Tribol. Lett.* **2006**, *21*, 245–252.
(51) Parry, E. J.; Tabor, D. *J. Mater. Sci.* **1973**, *8*, 1510–1516.

(52) Alexeev, A.; Verberg, R.; Balazs, A. C. *Langmuir* **2007**, *23*, 983–987.
(53) Schneider, F.; Draheim, J.; Kamberger, R.; Wallrabe, U. *Sens. Actuators, A* **2009**, *151*, 95–99.
(54) Lima, K.; Kimb, S.; Hahn, J. H. *Sens. Actuators, B* **2003**, *92*, 208–214.
(55) Kang, I.; Panneerselvam, D.; Panoskaltsis, V. P.; Eppell, S. J.; Marchant, R. E.; Doerschuk, C. M. *Biophys. J.* **2008**, *94*, 3273–3285.
(56) Lulevich, V.; Zink, T.; Chen, H.; Liu, F.; Liu, G. Y. *Langmuir* **2006**, *22*, 8151–8155.
(57) Alonso, J. L.; Goldmann, W. H. *Life Sci.* **2003**, *72*, 2553–2560.